Laboratory of pharmacology and molecular biology, Medical College, Henan University of Science and Technology, Luoyang, Henan Province, China

Differential expression of NAD(P)H oxidase isoforms and the effects of atorvastatin on cardiac remodeling in two-kidney two-clip hypertensive rats

Ruifang Li, Weijin Fang, Shanshan Cao, Yan Li, Jiangang Wang, Shoumin Xi, Bo Zhang, Yunxia He

Received September 10, 2012, accepted October 12, 2012

Rui-fang Li M.D. Professor of Pharmacology, Medical College, Henan University of Science and Technology, Anhui Road 31, Luoyang 471003, Henan Province, China
liruifang1234@yahoo.com.cn

Pharmazie 68: 261–269 (2013) *doi: 10.1691/ph.2013.2782*

The NADPH oxidases (Noxes) are a family of ROS (reactive oxygen species)-generating enzymes which play a critical role in the development of cardiac remodeling associated with heart failure. The Noxes of their catalytic isoforms include multiple homologues in cardiovascular cells with wide range tissue distribution. It is still unclear which Noxes represent the major enzymatic source of ROS in the heart and play a predominant role in cardiac hypertrophy. In this study we investigated the differential expression changes of NAD(P)H oxidase P47phox isoform and Nox homologues in left ventricle and the effects of atorvastatin on cardiac remodeling in two-kidney two-clip(2K2C) hypertensive rats. The mRNA and protein expression of Nox2, Nox4 and P47phox showed a sustained increase at 4, 8, 12 weeks after surgery in 2K2C rats. Administration of atorvastatin attenuated cardiac dysfunction, hypertrophy and fibrosis of 2K2C rats. However, atorvastatin treatment had no effects on BP regulation. Further studies revealed that atorvastatin inhibited the increased expression of Nox2, Nox4, P47phox as well as $O_2^{\bullet-}$ production in 2K2C hypertensive rats. These findings indicate that Nox2, Nox4 and P47phox play a crucial role in the development of cardiac remodeling in the 2K2C hypertensive rats. Atorvastatin, independent of BP control, exerts anti-remodeling effects partially by inhibition of NAD(P)H oxidase-mediated cardiac oxidative stress.

1. Introduction

Recent studies have demonstrated that cardiac remodeling was a risk factor of chronic heart failure (CHF). Previous data revealed that cardiac remodeling amelioration reduced cardiac morbidity and mortality (Zhao et al. 2008). To more effectively prevent cardiac hypertrophy and fibrosis and more effectively apply therapeutic intervention, it is important to understand the factors involved in ventricular growth both at the early and established stage of cardiac remodeling (Lee et al. 2006; Nabeebaccus et al. 2011). Angiotensin-converting enzyme inhibitors can lower blood pressure effectively, but they cannot reverse left ventricle (LV) mass in hypertensive rats completely (Thone et al. 2003), implying that other factors involved in cardiac remodeling.

The process of cardiac remodeling involved in complex molecular mechanisms, reactive oxygen species (ROS)-dependent pathways is the one of the mechanisms (Takimoto and Kass 2007; Kuroda and Sadoshima 2010). ROS exert biological effects by causing non-specific oxidative damage to DNA, proteins, lipids and macromolecules via specific regulation of cellular signaling pathways. Accumulating *in vitro* and *in vivo* evidence suggests that NADPH oxidases play important roles in the pathogenesis of cardiac remodeling (Hori and Nishida 2009; Brandes et al. 2010). The NADPH oxidases are a family of ROS (reactive oxygen species)- generating enzymes. NAD(P)H oxidase is composed by a membrane-bound heterodimer consisting a catalytic Nox2 subunit (also known as gp91phox) and a p22phox subunit and several cytosolic subunits (p47phox, p40phox, p67phox and Rac) that associate with the heterodimer in the activated enzyme. Five Nox isoforms form the basis of distinct NAD(P)H oxidase (Lambeth 2004). The Noxes of their catalytic isoforms include multiple homologues in cardiovascular cells with wide range tissue distribution: Nox1, Nox2, Nox4, Nox5, etc. The two main isoforms expressed in the heart are Nox2 and Nox4. Nox4 binds to P22phox forming a heterodimer and appears to be constitutionally active, however, Nox2 requires any other regulatory subunit such as P47phox or p22phox (Sedeek et al. 2009; Kuroda et al. 2010). Although the hypothesis that different Nox enzymes are involved in different pathophysiological developments is supported by some *in vitro* and *in vivo* studies (Looi YH et al. 2008; Brandes et al. 2010), very little is known, however, about the mechanism. There is a paucity of information on the regulation, signaling and function of these Nox family members. The study on the regulation and function of Nox isoforms in the development of cardiac hypertrophy can provide new inhibitors which target Nox isoforms in special kind cardiovascular disease.

3-Hydroxy-3-methylglutaryl coenzyme A (HMG-CoA) reductase inhibitors have been shown to reduce cardiovascular morbidity and mortality far surpassing as a cholesterol-lowering drug to treat hyperlipidemia (Habibi et al. 2007; Tajima et al. 2008). In a chronic angiotensin (Ang) II-infusion model and in spontaneously hypertensive rats (SHR), treatment with statins suppressed production of ROS and reduced cardiovascular derangements (Dechend et al. 2001; Sicard et al. 2008). However, in the Ang II-infused model treated with statin, only the Nox4 mRNA level was reduced while in the ApoE-deficient mice fed a high-fat diet, treatment with atorvastatin did not

alter the mRNA level of Nox1 but decreased the levels of other Nox isoforms, Nox2 and Nox4 (Cui et al. 2009). These findings suggest that NADPH oxidase is a crucial target of statin therapy. The results of our preliminary experiments showed that different Nox homologues exhibited different expression pattern in left ventricle (LV) and aorta. The protein expression and mRNA transcription of Nox2 and Nox4 increased in LV, while that of Nox1 and Nox4 increased significantly in aorta in 2K2C hypertensive rats 6 weeks after operation (Wang et al. 2007). In this study, renovascular hypertensive rats were used to investigate the differential expression of NADPH oxidase isoforms, which may help to find the special NADPH oxidase isoform in the development of cardiac hypertrophy and understand the multiplicity of biological functions of these oxidases. Further, we will investigate the effects of atorvastatin on two-kidney, two-clip (2K2C) renovascular hypertension-induced cardiac remodeling in rats and its mechanism related to NAD(P)H oxidase.

2. Investigations and results

2.1. Hemodynamic parameters and LVW/BW ratio 4, 8 and 12 weeks after the operation in 2K2C rats

To investigate the hemodynamic change and cardiac hypertrophy in 2K2C rats of different age and the effects of atorvastatin, a two-kidney, two-clip (2K2C) renovascular hypertensive model was established and cardiac hemodynamic parameters were examined in rats. The ratio of left ventricle weight (LVW) to body weight (BW) was analyzed as a surrogate marker of hypertension-induced left ventricular hypertrophy.

Compared with age-matched Sham rats, the left ventricle end-systolic pressure (LVESP), left ventricle end-diastolic pressure (LVEDP) and LVW/BW were increased progressively in 2K2C rats at 4 weeks, 8 weeks and 12 weeks after the surgery, which indicated that both preload and afterload were increased and left ventricle remodeling occurred in 2K2C rats (Table 1). In contrast, compared with the age-matched Sham group, the maximum ascending and declining rate of left ventricular pressure (± dp/dtmax) decreased significantly in 2K2C rats at 8 w and 12 w after surgery respectively, indicating that contractility and diastolic compliance of the heart were decreased. However, + dp/dtmax has not significantly decreased in 2K2C rats at 4 weeks after operation, suggesting that the left ventricle diastole dysfunction is sooner than left ventricular systolic dysfunction.

2.2. Effects of atorvastatin on hemodynamic parameters and LVW/BW ratio

As shown in Table 2, Aortic systolic pressure (AoSP), aortic diastolic pressure (AoDP), LVESP, LVEDP and LVW/BW increased while ±dp/dtmax decreased significantly in a time-dependent manner in 2K2C rats compared with Sham rats. Treatment with candesartan for 4 weeks markedly decreased LVW/BW, LVEDP and ± dp/dtmax of 2K2C rats, which exhibited improvement of cardiac hypertrophy, left ventricular systolic function and diastolic compliance. However, there was no significant change of AoSP, AoDP and LVESP in AtoH and AtoL compared with those in 2K2C rats. These results indicated that atorvastatin treatment might exert cardioprotective effects independent of BP control. But atorvastatin decreased LVEDP and elevated -dp/dtmax significantly more than its effects on LVESP and + dp/dtmax, indicating that atorvastatin decreased the afterload better than the preload and improved cardiac diastolic function more remarkable than cardiac systolic function.

2.3. Morphometric analysis of left ventricular myocardium at 4, 8 and 12 weeks after operation and effects of atorvastatin

Morphometric analysis of LV sections from different treatment groups was performed by using HE staining (Fig. 1). HE stain-

Table 1: Changes of hemodynamic parameters and the ratio of LVW/BW in rats

Parameters	4 w		8 w		12w	
	Sham	2K2C	Sham	2K2C	Sham	2K2C
LVESP (mmHg)	103 ± 5.3	170 ± 7.9*	107 ± 11	180 ± 10*	105 ± 8.8	189 ± 10.1*
LVEDP (mmHg)	3.34 ± 0.7	5.5 ± 1.1*	3.09 ± 0.6	8.3 ± 1.8$^{*\#}$	4.03 ± 0.5	11.8 ± 1.5$^{*\Delta}$
+ dp/dt$_{max}$(mmHg/s)	4.9 ± 0.8	4.3 ± 0.5	5.2 ± 0.6	2.8 ± 0.5$^{*\#}$	5.0 ± 0.8	1.9 ± 0.4$^{*\Delta}$
−dp/dt$_{max}$(mmHg/s)	4.6 ± 0.5	3.7 ± 0.3*	4.7 ± 0.7	2.5 ± 0.3$^{*\#}$	4.3 ± 0.6	1.5 ± 0.2$^{*\Delta}$
LVW (mg)	278 ± 38	361 ± 47*	443 ± 60	703 ± 30*	592 ± 28	1000 ± 66$^{*\Delta}$
BW(g)	183 ± 12	176 ± 12	293 ± 15	301 ± 13	377 ± 22	353 ± 25$^{\Delta}$
LVW/BW (mg/g)	1.5 ± 0.1	2.0 ± 0.3*	1.5 ± 0.1	2.3 ± 0.2*	1.6 ± 0.1	2.8 ± 0.2$^{*\Delta}$

Values are means ± SD. n = 10 in each group. LVESP, Left ventricular end-systolic pressure; LVEDP, Left ventricular end-diastolic pressure; + dP/dtmax, maximum ascending rate of left ventricular pressure; -dP/dtmax, maximum declining rate of left ventricular. LVM, left ventricular weight; BW, body weight; LVW/BW, ratio of left ventricle weight to body weigh; 4 w, 4 weeks after operation; 8 w, 8 weeks after operation; 12 w, 12 weeks after operation. $^{*}p < 0.05$ vs. age-matched Sham group; $^{\#}p < 0.05$ vs. 2K2C 4w group; $^{\Delta}p < 0.05$ vs. 2K2C 8w group.

Table 2: Effects of atorvastatin on hemodynamics and ratio of LVW/BW

parameters	Sham	2K2C	AtoH	AtoL	Can
AoSP (mmHg)	109.0 ± 8.7	177.0 ± 4.5*	160.0 ± 4.2$^{\Delta}$	167.0 ± 5.1$^{\Delta}$	113.0 ± 9.2$^{\#}$
AoDP (mmHg)	83.0 ± 4.5	142.0 ± 7.6*	134.0 ± 8.0$^{\Delta}$	138.0 ± 6.0$^{\Delta}$	94.9 ± 6.5$^{\#}$
LVESP (mmHg)	104.0 ± 4.5	171.0 ± 11.9*	163.0 ± 16.5$^{\Delta}$	167.0 ± 14.0$^{\Delta}$	107.0 ± 4.8$^{\#}$
LVEDP (mmHg)	4.8 ± 0.8	9.2 ± 1.3*	6.2 ± 1.0$^{\#\Delta}$	7.1 ± 0.8$^{\#\Delta}$	5.1 ± 0.6$^{\#}$
+ dp/dt$_{max}$ (mmHg/s)	3.5 ± 0.3	1.7 ± 0.1*	2.9 ± 0.5$^{\#}$	2.3 ± 0.2$^{\#\Delta}$	3.2 ± 0.2$^{\#}$
−dp/dt$_{max}$ (mmHg/s)	3.5 ± 0.4	1.4 ± 0.2*	3.6 ± 0.3$^{\#}$	2.7 ± 0.3$^{\#\Delta}$	3.3 ± 0.2$^{\#}$
LVW/BW (mg/g)	1.5 ± 0.1	2.4 ± 0.2*	1.7 ± 0.2$^{\#}$	1.9 ± 0.3$^{\#}$	1.6 ± 0.3$^{\#}$

Values are means ± SD. n = 10 in each group. AoSP: Aortic systolic pressure; AoDP: Aortic diastolic pressure; Other abbreviations were shown as in Table 1; Sham, Sham- operation group; 2K2C, two kidney two clip group; AtoH, high dose of atorvastatin group; AtoL, low dose of atorvastatin group; Can, candesartan group. $^{*}p < 0.05$ vs. Sham group; $^{\#}p < 0.05$ vs. 2K2C group; $^{\Delta}p < 0.05$ vs. Can group.

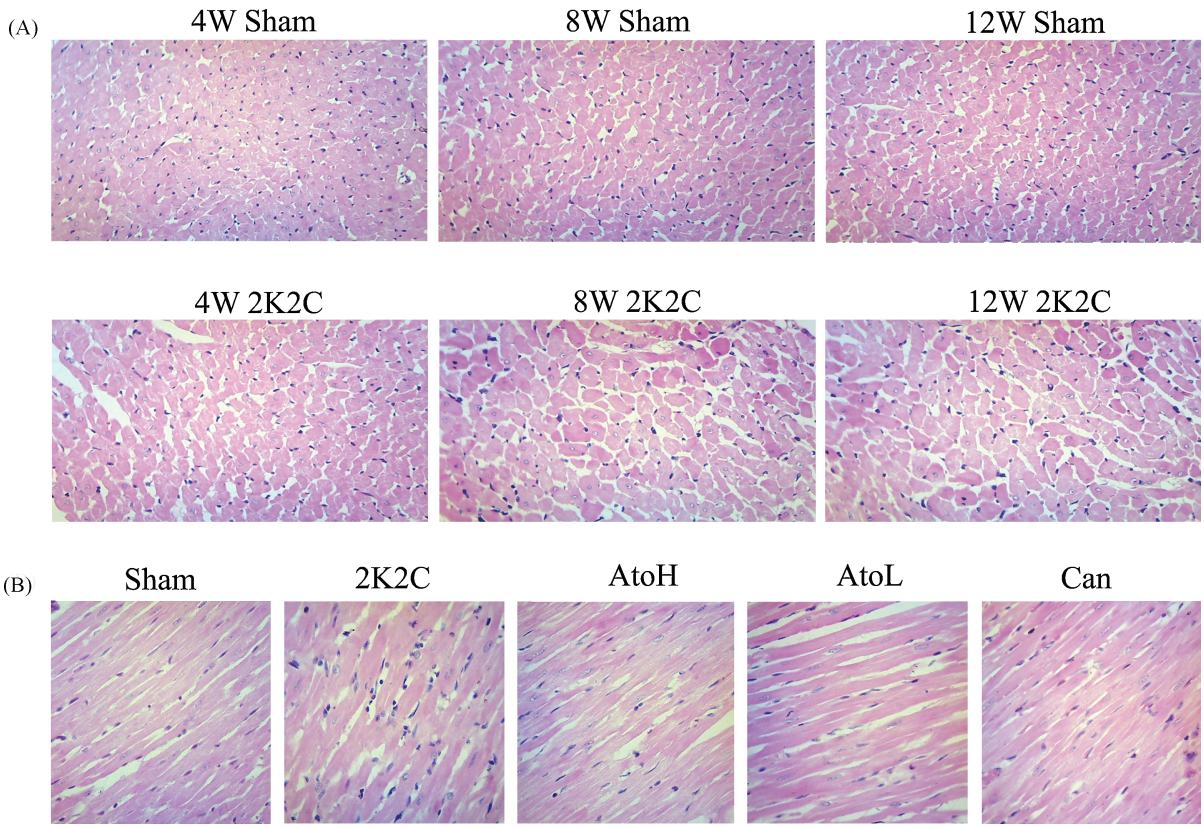

Fig. 1: HE staining of left ventricular myocardium at 4, 8 and 12 weeks after operation and the effect of atorvastatin (magnification × 200). (A) Representative pictures of cardiomyocyte cross sections of LV with HE staining at different time after the operation. (B) Representative pictures of cardiomyocyte longitudinal sections of LV with HE staining. Both atorvastatin and candesartan treatment for 4 weeks attenuated myocardial hypertrophy and disordered arrangement in LV of 2K2C rats. Abbreviations as above

ing showed that cardiomyocyte transection diameter (TDM), cardiac hypertrophy increased significantly and muscle cells showed disordered arrangement in LV of 2K2C rats at 4w, 8w and 12 w after the operation (Fig. 1A). However, cardiomyocyte hypertrophy and disordered arrangement were markedly attenuated by atorvastatin and candesartan treatment for 4 weeks in LV of 2K2C rats. These data demonstrated that both atorvastatin and candesartan ameliorated remarkably the cardiac cardiomyocyte hypertrophy of 2K2C hypertensive rats (Fig. 1B).

2.4. Left ventricular and perivascular fibrosis in 2K2C rats and protection effects of atorvastatin

To investigate the effect of atorvastatin on cardiac fibrosis, VG staining was used to detect the content of cardiac muscle collagen. As shown in Fig. 2, diffuse interstitial and perivascular fibrosis were evident in 2K2C hypertensive rats, which were also demonstrated by the much greater collagen volume fraction (CVF) and perivascular collagen area (PVCA) in 2K2C rats. Atorvastatin treatment for 4 weeks ameliorated the severe fibrosis, both in the interstitium and perivascular, reflected by the decreasing CVF and PVCA.

2.5. Changes of ANF and β-MHC mRNA expression 4, 8 and 12 weeks after operation in LV of 2K2C rats and the effects of atorvastatin

To further confirm the degree of ventricular hypertrophy, RT-PCR was used to evaluate the mRNA expression of the atrial natriuretic factor (ANF) and cardiac β-myosin heavy chain (β-MHC) in LV. ANF and β-MHC were markedly increased in 2K2C rats in a time-dependent manner compared with the age-matched sham- operated group. Atorvastatin and candesartan treatment for 4 weeks decreased significantly ANF and β-MHC mRNA expression in LV of 2K2C hypertensive rats (Fig. 3).

2.6. Changes of Nox2, Nox4 and p47phox expression 4, 8 and 12 weeks after operation in LV of 2K2C rats and the effects of atorvastatin

To identify the changes of NAD(P)H oxidase isoforms involved in cardiac hypertrophy, we examined the expression of p47phox, Nox2 and Nox4 in 2K2C rats at 4, 8 and 12 weeks after operation using RT-PCR and Western blot. The expression of p47phox, Nox2 and Nox4 increased in LV of 2K2C hypertensive rats in a time-dependent manner. However, these isoforms expression decreased significantly after 4 weeks administration of atorvastatin and candesartan compared with the 2K2C group (Fig. 4).

2.7. Enhanced generation of $O_2^{\bullet-}$ in LV in 2K2C rats was down-regulated by atorvastatin

To investigate the mechanism by which atorvastatin attenuated cardiac remodeling and improved the hemodynamics, we examined its effect on the $O_2^{\bullet-}$ production, frozen tissue sections of LV were treated with diphenylene iodonum (DPI, 10 μmol/L). The addition of DPI significantly inhibited $O_2^{\bullet-}$ production in LV from 2K2C rats, which means that NAD(P)H oxidase may contributed to the enhanced generation of $O_2^{\bullet-}$ and over-oxidative stress.

As shown in Fig. 5, $O_2^{\bullet-}$ formation evaluated by the oxidative fluorescence dye DHE in the left ventricle was greater in the 2K2C hypertensive group than in the Sham group. Atorvastatin suppressed $O_2^{\bullet-}$ formation to normal levels. DPI treatment in

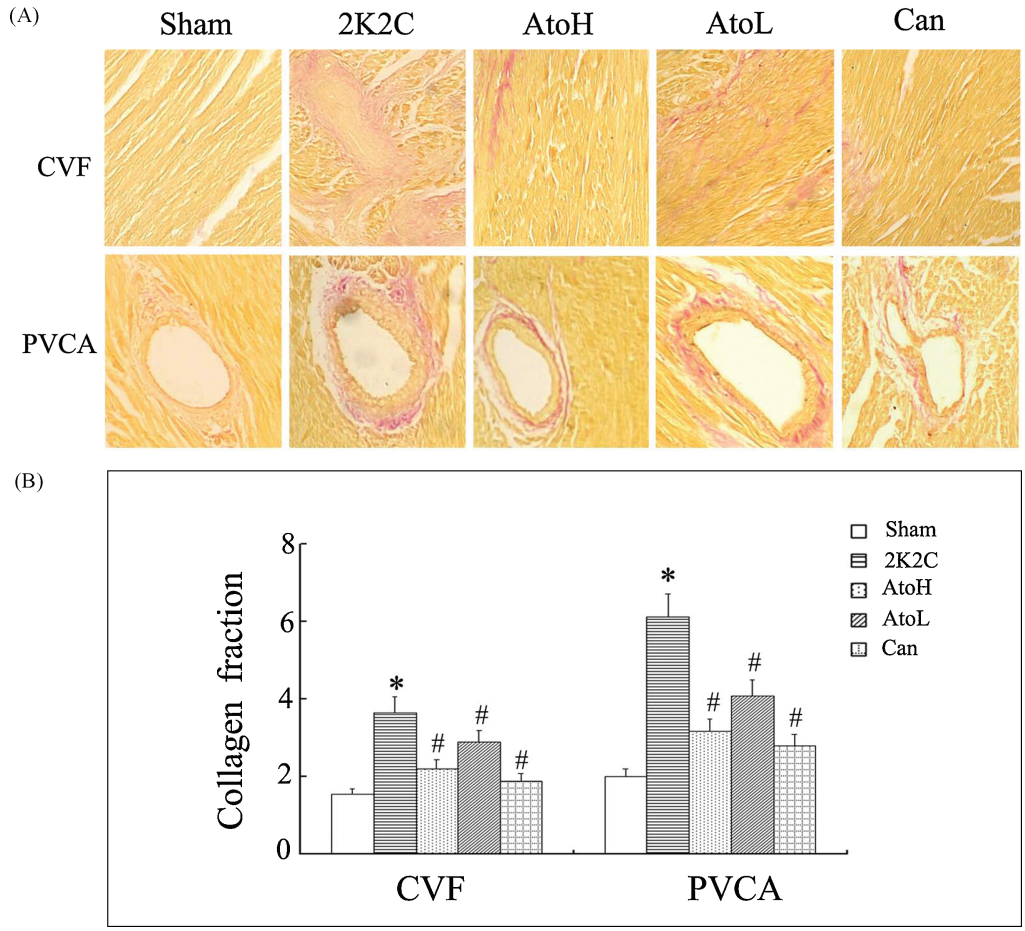

Fig. 2: Left ventricular myocardium interstitial and perivascular fibrosis in 2K2C hypertensive rats and the effect of atorvastatin. (A) Representative pictures of myocardial and perivascular fibrosis with the collagen-specific dye method Van Gieson (VG) staining, in which collagen fibers appeared as red structures, and myocytes and intramyocardial vessels were yellow (magnification ×200); (B) Collagen deposition in the interstitial and perivascular regions of the LV, expressed as collagen volume fraction (CVF) and perivascular collagen area (PVCA) measured by videodensitometry. Abbreviations as above. Data are expressed as means ± S.D., n = 10. *$p < 0.05$ vs. sham group. #$p < 0.05$ vs. 2K2C group

the 2K2C hypertensive group (DPI) also significantly decreased $O_2^{\bullet -}$ formation in the LV, even significantly lower than the normal levels, which demonstrated that NAD(P)H oxidase was the major sources of $O_2^{\bullet -}$ production in left ventricle.

3. Discussion

In this study, we found that Nox2, Nox4 and P47phox expression have been shown increasing in LV with the progression of the cardiac hypertrophy. We also demonstrated that atorvastatin attenuated cardiac hypertrophy in 2K2C rats, independent of the blood pressure changes via a NAD(P)H oxidase-dependent pathway. Our findings are supported by the following results: (1) 2K2C renovascular hypertension was associated with the development of ventricular hypertrophy confirmed by LVW/BW, histological cardiomyocyte size, ANF and β-MHC mRNA expression of LV and hemodynamic parameters. (2) The expression of Nox2, Nox4 and p47phox maintained stable increasing with the progression of the cardiac hypertrophy, indicating that NAD(P)H oxidase are directly related to the cardiac hypertrophy. (3) NAD(P)H oxidase plays a key role in promoting the pathogenesis of ventricular hypertrophy in 2K2C renovascular hypertension, which can be reversed by administration of atorvastatin and candesartan. (4) Atorvastatin prevents the progression of ventricular hypertrophy by inhibiting NAD(P)H oxidase and $O_2^{\bullet -}$ production in LV in 2K2C renovascular hypertension rats.

Myocardial remodeling is characterized by alterations in left ventricular size, shape and wall thickness (Weber 1997; Wang et al. 2011). Growing evidence suggests that oxidative stress mediated by reactive oxygen species plays a role in the pathogeneses of myocardial remodeling (Giordano 2005; Maejima et al. 2011). Reactive oxygen species (ROS)-dependent signaling is implicated in cardiac stress responses, but the role of different ROS sources remains unclear. Vascular NAD(P)H oxidases are the major enzymatic sources of ROS in the heart (Lambeth 2004). Recent studies suggested that NAD(P)H plays an essential role in the development of hypertension, cardiac hypertrophy and interstitial fibrosis (Murdoch et al. 2006). In the present study, the expression of Nox2, Nox4, and p47phox isoform of NAD(P)H oxidase increased significantly 4 weeks after surgery and the expression levels of these isoforms maintained stable increasing with the progression of the cardiac hypertrophy 8, 12 weeks after operation, indicating that NAD(P)H oxidase is directly related to the development of cardiac hypertrophy, the Nox2 and Nox4 might be the major isoform involved in ROS production and LV remodeling in 2K2C renovascular hypertension rats. Meanwhile it is known that p47phox also plays an important effect in this hypertension model. Earlier studies suggest that the different subunits of NAD(P)H oxidase may mediate various effects on cardiac remodeling (Sumimoto et al. 2005; Wang et al. 2007). Nox2 was thought as the major isoform to take part in cardiac hypertrophy and interstitial fibrosis (Bendall et al. 2002). Nox4 in cardiomyocytes is a major source of mitochondrial oxidative stress, thereby mediating cardiac dysfunction during pressure overload. Unlike other Nox proteins, Nox4 activity is regulated mainly by its expression level,

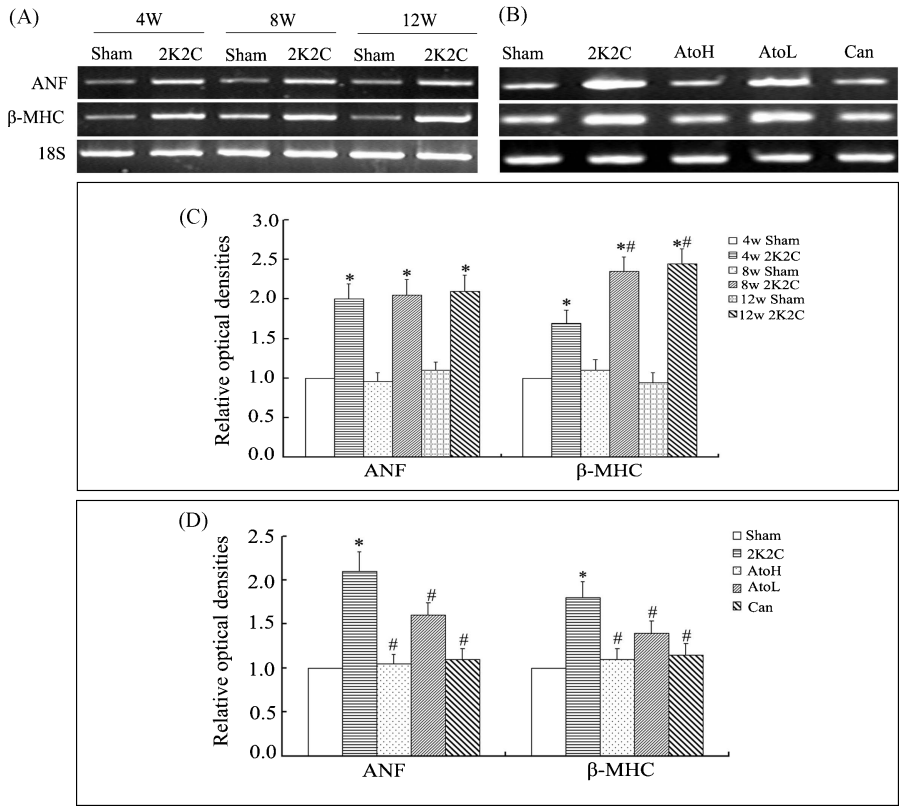

Fig. 3: Changes of the mRNA expression of ANF and β-MHC in left ventricle of 2K2C rats at 4, 8 and 12 weeks after the operation and the effect of atorvastatin. (A) Representative PCR band photograph of levels of ANF and β-MHC mRNA in left ventricle of 2K2C rats at different time. (B) Effect of atorvastatin on ANF and β-MHC mRNA expression in left ventricle of 2K2C rats treated for 4 weeks. (C and D) Fold of the mRNA expression of ANF and β-MHC to sham group in left ventricle. The data are presented as fold of optical densities to 18S, relative to sham group. Data are means ± SD, n = 6. *$p < 0.05$ vs. age matched sham group. #$p < 0.05$ vs. 4w 2K2C group. (C); *$p < 0.05$ vs. sham group. #$p < 0.05$ vs. 2K2C group (D). Sham, sham-operation group; 2K2C, 2K2C-operation group; AtoH, high dose of atorvastatin (10 mg/kg/day); AtoL, low dose of atorvastatin (5 mg/kg/day), Can, candesartan (10 mg/kg/day)

which increases in cardiomyocytes under stresses such as pressure overload or hypoxia (Kuroda et al. 2010). Cardiomyocyte Nox4 is a unique inducible regulator of myocardial angiogenesis, a key determinant of cardiac adaptation to overload stress (Martyn et al. 2006; Zhang et al. 2010). The two-kidney, two-clip (2K2C) rat model employed in our experiment is an ideal model for studying the role of volume expansion and pressure-overload in the development of hypertension. In this renovascular hypertension model, plasma Ang II levels increased, excessive oxidant stress was present in the heart (Sun and Zhang 2005). Our results suggest that both Nox2 and Nox4 are the key determinants of cardiac remodeling of renovascular hypertension.

NADPH oxidases might be considered important targets for the prevention and treatment of 2K2C hypertension-induced cardiac remodeling. In this study, the amelioration effects of atorvastatin on cardiac remodeling were clearly demonstrated in 2K2C model. We also found that atorvastatin cannot decrease the systolic blood pressure to normal levels, indicating that atorvastatin treatment might exert cardioprotective effects independent of BP control. Our present findings suggest that atorvastatin has direct tissular effects dissociated from its hemodynamic effects. Recent studies also reported that a dissociation between the effects of blood pressure and cardiac structure existed (Lee et al. 2006; Xu Z et al. 2008; Wang et al. 2011). Administration of statins resulted in reduced generation of the superoxide anion and inhibited myocardial hypertrophy and cardiac fibrosis in the heart by decreasing activity of NAD(P)H oxidase (Takayama et al. 2004; Sicard et al. 2008). Interestingly, we found that atorvastatin decreased left ventricle end-diastolic pressure (LVEDP) effectively, indicating that atorvastatin decreased the afterload better than the preload, improving the diastolic function even more significantly, also can better improve heart compliance and delay the deterioration of the cardiac function. In this study, we found that candesartan (the positive control drug), a typical AT1 antagonist, indeed significantly lowered BP, attenuated cardiac hypertrophy, through mechanisms including decreased $O_2^{\bullet -}$ production associated with down-regulation of NAD(P)H oxidase, a result that agrees with previous findings (Schiffrin 2002; Wang et al. 2007).

We presently demonstrated that atorvastatin markedly attenuated the development of cardiac remodeling, and this effect was accompanied by reduced production of $O_2^{\bullet -}$ and expression of NAD(P)H oxidase. Beneficial effects of statins on cardiovascular diseases have been attributed to decreased generation of reactive oxygen species (ROS) (Whaley-Connell et al. 2008; Cui et al. 2009). Various studies have demonstrated that ROS play an essential role in the development of renovascular hypertension by disrupting normal signaling pathways (Wang et al. 2007; Polizio 2008). Our results showed that atorvastatin down-regulated the expression of Nox4 and p47phox mRNA and protein in LV of 2K2C hypertensive rats. The decrease in the expression of Nox4 and p47phox brought about by atorvastatin may be contributed to the reduced generation of $O_2^{\bullet -}$ in 2K2C rats, and then delay the development of myocardial hypertrophy. In line with our findings, it was reported that treatment with pitavastatin suppressed vascular Nox4 expression in an animal model of congestive heart failure and atorvastatin down-regulated the expression of Nox4 mRNA in the Ang II–infused model as well as in ApoE-deficient mice fed a high-fat diet (Cui et al. 2009).

In summary, the expression of Nox2 and Nox4 might account for the increased formation of $O_2^{\bullet -}$ regulated by NAD(P)H oxidase in the 2K2C model, which contributes to the devel-

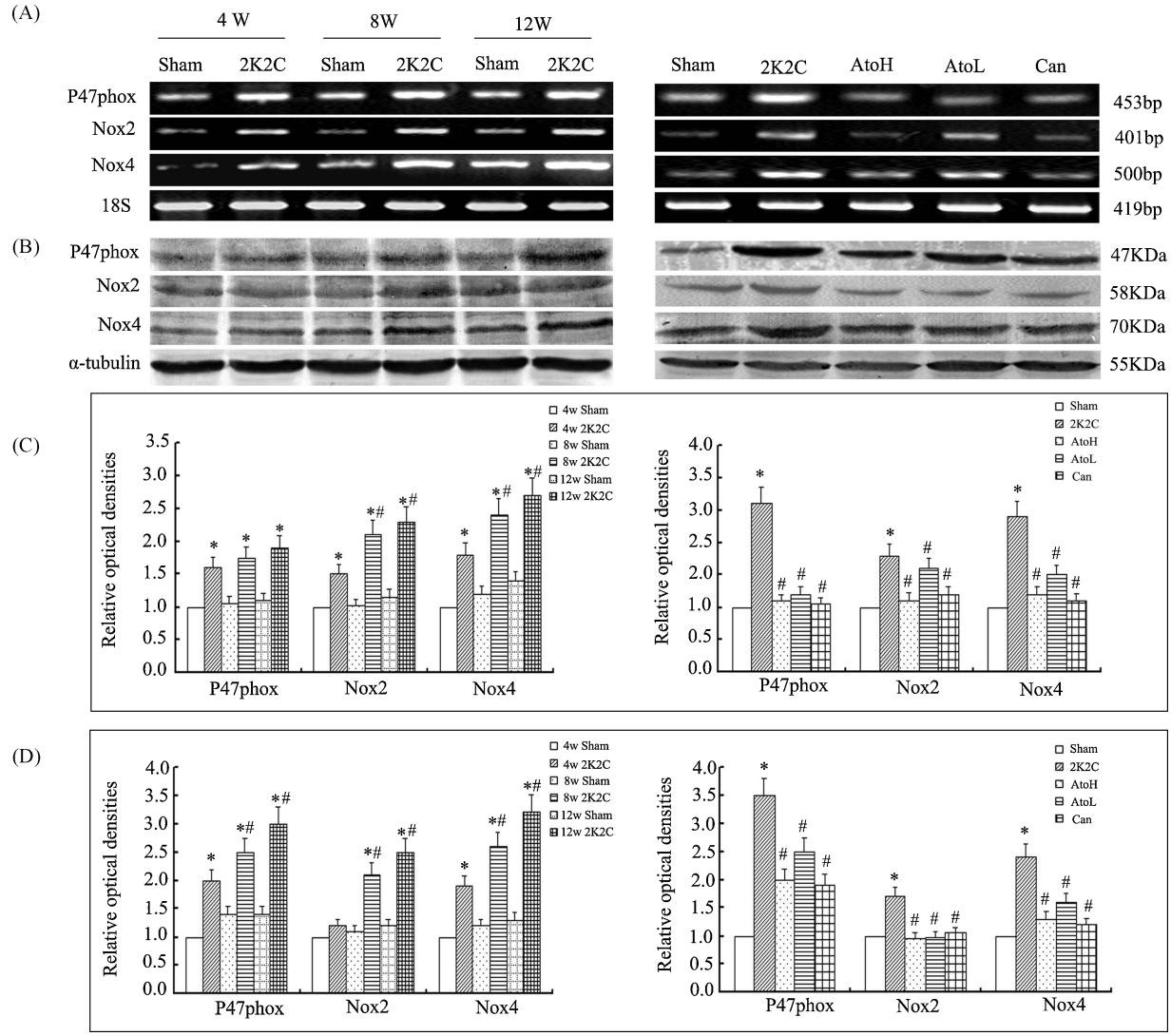

Fig. 4: Changes of p47phox, Nox2 and Nox4 expression at 4, 8 and 12 weeks in LV of 2K2C rats and the effect of atorvastatin. The mRNA and Protein expression were examined via RT-PCR and Western blot analysis. (A) Representative PCR band photograph. (B) Original Western blots representing the similar results of 6–10 rats. Equal protein loading was verified by α-tubulin immunostaining. (C) Ratio of the mRNA expression of p47phox, Nox2 and Nox4 to α-tubulin in the LV. (D) Densitometric quantification of Western blots in LV. The values from experiment groups have been normalized to values in sham group. Abbreviations as above. Data are means ± SD, n = 6. *$p < 0.05$ sham group. #$p < 0.05$ vs. 2K2C group

opment of renovascular hypertension and subsequent cardiac remodeling. The findings suggest a pathogenetic role of NAD(P)H oxidase in promoting the initiation and progression of cardiac remodeling. Atorvastatin attenuated cardiac remodeling and cardiac dysfunction in 2K2C rats by inhibiting NAD(P)H oxidase-derived ROS and redox-signaling, independent of hemodynamic changes. Treatment aimed at inhibition of NAD(P)H oxidase could have advantages over current therapy for cardiac remodeling. The present study provides direct evidence for the differential expression of Nox2, Nox4 and P47phox in cardiac remodeling in 2K2C hypertension model rats and evaluates the inhibitory effect of atorvastatin on cardiac remodeling in this model. These results may have important therapeutic implications.

4. Experimental

4.1. Experimental animals and groups

Experimental protocols followed standards and policies of the Henan University of Science and Technology's Animal Care and Use Committee and complied with the National Institutes of Health Guide for the Care and Use of Laboratory Animals. Renovascular hypertension was induced in rats using the two-kidney two-clip (2K2C) method as previously described (Wang et al. 2007). Briefly, male Sprague–Dawley rats 100 ± 20 g were anaesthetized with sodium pentobarbital (30 mg kg^{-1}, i.p.). Titanium alloy clips, 0.3 mm internal diameter, were slipped around the left and right renal artery as close as possible to its exit from the aorta. Sham-operated rats were exposed to the same surgical manipulations, except the clipping. The wound was sutured, and the animals were allowed to recover. After return to their cage, all rats were maintained on a regular diet for 4 weeks.

Four weeks after the both sides renal artery were clipped, rats that SBP was higher than 160 mmHg were randomly divided into three groups: 4 week group (4w 2K2C), 8 week group (8w 2K2C), 12 week group (12w 2K2C) after operation. Correspondingly, the sham-operated control rats were divided into three groups: 4 week group (4w Sham), 8 week group (8w Sham), 12 week group (12w Sham) after operation. In the experiment of atorvastatin anti-remodeling effects, the 2K2C hypertensive rats of 4 weeks after operation were divided into untreated (2K2C) and atorvastatin treated (AtoH, AtoL) and candesartan treated (Can) groups. Atorvastatin (10 mg kg^{-1} or 5 mg kg^{-1} per day, mixed with sodium chloride), candesartan (10 mg kg^{-1} per day, mixed with sodium chloride) was given by gastric gavage once a day for 4 weeks. The sham-operated rats were orally given vehicle (sodium chloride), which served as control.

4.2. Hemodynamic analyses

Functional parameters were measured in anesthetized rats at the end of the study. LV hemodynamic studies were performed by cannulation of the right carotid artery with a polyethylene Millar Pressure Catheter that was carefully advanced to the LV (Zhou et al. 2006). Then the rats were sacrificed and the hearts were harvested. The left ventricle was separated from the

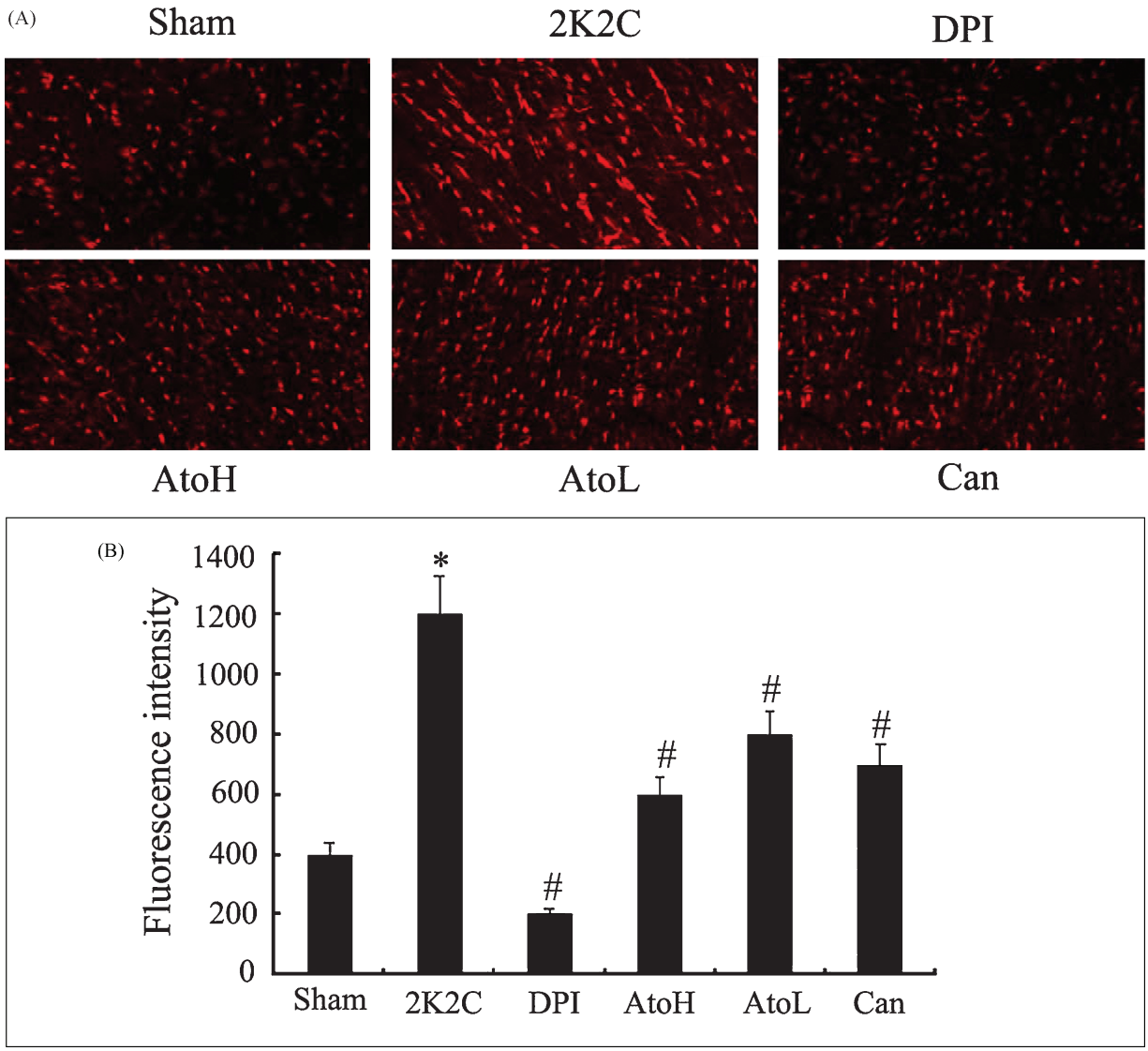

Fig. 5: Enhanced generation of $O_2^{\bullet-}$ in LV in 2K2C rats and the effect of atorvastatin. In situ basal $O_2^{\bullet-}$ levels in aorta measured by laser confocal fluorescent microscopy. (A) Fluorescent photomicrographs of aortic sections incubated with the superoxide-sensitive dye DHE (red fluorescence when oxidized to ethidium bromide by superoxide). (B) Quantification of oxidative fluorescence intensity. DPI, Heart freezing section of 2K2C hypertensive rats were treated with diphenylene iodium at concentration of 10 μmol/L for 30 min before they were incubated with DHE. Other abbreviations as above. Data are means ± S.D., representative of similar results obtained from 6–8 rats. *$p < 0.05$ sham group. #$p < 0.05$ vs. 2K2C group

atrium and the right ventricle. Then, they were weighed. In addition, total body weight (BW) was obtained before initiation of treatment and at the time the animals were killed. Cardiac hypertrophy was assessed by measuring the ratio of the LV wet weight to total body weight (LVW/BW). The left ventricle was frozen in liquid nitrogen and stored at −80 °C until use.

4.3. Morphometric determination

The LV myocardium was fixed in 10% formalin. Tissues were dehydrated, embedded in paraffin blocks, cut into 5 μm sections, and mounted on 3-aminopropyltriethoxysilane-coated slices. Sections were deparaffinized, rehydrated, and washed with H_2O and stained with hematoxylin-eosin (HE) for assessment of myocardial hypertrophy by measuring cardiomyocyte diameter under a light microscope × 200 magnification.
Additionally, the cardiac sections were stained with VG staining for assessment of interstitial and perivascular collagen content. Collagen density was evaluated in 10 fields in each region of the heart (magnification × 200) from three nonconsecutive serial sections. Quantification of fibrosis was performed using an image analysis system (Northern Eclipse 5.0; EM-PIX Imaging Inc).

4.4. VG staining and collagen quantification

LV tissues sections were deparaffinized, rehydrated, and washed with H_2O. The sections were stained with 1% acid fuchsin and 0.5% saturated picric acid (Van-Gieson staining, VG staining) for assessment of interstitial and perivascular collagen content. Quantification of fibrosis was performed using an image analysis system (Northern Eclipse 5.0; EM-PIX Imaging Inc). A single investigator unaware of the nature of the experimental groups performed the analysis.

4.5. Reverse transcription–polymerase chain reaction analysis

Total RNA was isolated from the frozen left ventricles and aortas using TRIzol reagent according to the manufacturer's instructions (Invitrogen, Carlsbad, CA) as previously described (Zhang et al. 2007). Total RNA (0.5−1 μg) was reverse transcribed and amplified using the RNA PCR Kit (Takara Bio Inc.) with the primers listed in Table 3 under the following reaction conditions: 95 °C for 5 min, then different cycles consisting of 30 s at 95 °C, 30 s at 62 °C and 50 s at 72 °C, and 72 °C for 10 min. The PCR product was separated using electrophoresis on 1.5 % agarose gel and semi-quantified as a ratio to 18S. DL-2000 marker (TaKaRa) was used as a size standard.

4.6. Western blot analysis

Primary antibodies to P47phox (sc-17845), Nox2 (sc-27635), Nox4 (sc-30141) were purchased from Santa Cruz Biotechnology. Immunoblots were basically performed as previously described (Zhang et al. 2007). The isolated LV were quickly frozen in liquid nitrogen, and homogenized with a motorized homogenizer in ice-cold lysis buffer containing protease inhibitors (50 mmol/L Tris/HCl, pH 7.4, 1 mmol/L EDTA, 500 mmol/L phenylmethylsulfonyl fluoride (PMSF), 2 mmol/L leupeptin, and 10 mg/mL aprotinin), centrifuged, then the supernatants were collected. Protein concentrations

Table 3: Oligonucleotide primer sequences for NAD(P)H isoforms, ANF, β-MHC and 18S

mRNA	Primer sequence (5′–3′)	Cycles	Product sizes (bp)
P47phox	Forward: CCACACCTCTTGAACTTC Reverse: GCCATCTAGGAGCTTATG	35	453
Nox2	Forward:TATTGTGGGAGACTGGACTG Reverse: GATTGGCCTGAGATTCATCC	35	401
Nox4	Forward: GTTCCAAGCTCATTTCCCAC Reverse:GTATCGATGCAAACGGAGTG	35	500
ANF	Forward: AAGCTGTTGCAGCCTAGTCC Reverse:CTGCTAGACCACCTGGAGGA	30	320
β-MHC	Forward:TTGACAGAACGCTGTGTCTCCT Reverse: CACTCAACGCCAGGA	30	544
18S	Forward: CACCTACGGAAACCTTGTTAC Reverse:GTCCCCCAACTTCTTAGAG	30	419

were determined by the method of Bradford (BioRad, Hercules, CA, USA). Equal amounts of protein (60 μg protein per lane) were separated by 12% SDS-PAGE and then transferred onto PVDF membranes (Bio-Rad, Hercules, CA, USA). Blocking solution (5% skim milk) was loaded over membranes for 1 h at room temperature. The membranes were incubated with anti-p47phox, anti-Nox2, anti-Nox4 antibody (1:200 dilution respectively) overnight at 4 °C and with anti-tubulin antibody (1:10,000 dilution, Sigma) at 4 °C overnight, then incubated with responding horseradish peroxidase-labeled secondary antibodies at room temperature for 1 h. The signals were detected by the enhanced chemiluminescence method. Quantitation of protein band density, normalized to α-tubulin band density, was performed using Gel-Pro Analyzer 4.0. Data are reported as normalized protein band density.

4.7. NAD(P)H oxidase-dependent superoxide production

The oxidative fluorescence dye dihydroethidium was used to evaluate *in situ* $O_2^{\bullet-}$ generation in the LV as described previously (Wang et al. 2007). In brief, unfixed frozen samples embedded in optimal cutting temperature (OCT) compound was cut in 30 μm thick sections which were placed on glass slides, augmented with dihydroethidium (10 μmol/L), and then capped with coverslips. The slides were incubated in a light-protected humidified chamber at 37 °C for 30 min. The oxidative fluorescence intensity was detected by a laser scanning confocal imaging system (Olympus FV500). Superoxide levels were also measured in the presence of 10 μM diphenylene iodium (DPI), a selective inhibitor of NAD(P)H oxidase. A double-blind design was used to evaluate the image intensity. The highest and average fluorescent intensities were used for image quantification.

4.8. Statistical analysis

Results are presented as means ± S.D. Unpaired t-test, one-factor ANOVA followed by Student's Newman–Keul's test, and linear correlation tests were used. P value < 0.05 was considered statistically significant.

Acknowledgements: This work was supported by National Natural Science Fund of China (No: 30772576); Key Natural Science Fund of People's Government of Henan Province, PR of China (No: 082201170001); Innovation Fund of Henan University of Science and Technology (2009CZ0008). We thank Mr. Xie Xiaoyan and Mr. Fu Yinfeng for their excellent technical supports and Dr Gao Jie and Wang Ping for their proof reading the article.

References

Brandes RP, Weissmann N, Schröder K (2010) NADPH oxidases in cardiovascular disease. Free Radic Biol Med 49: 687–706.

Bendall JK, Cave AC, Heymes C, Gall N, Shah AM (2002) Pivotal role of a gp91 (phox)-containing NADPH oxidase in angiotensin II-induced cardiac hypertrophy in mice. Circulation 105: 293–296.

Cui W, Matsuno K, Iwata K, Ibi M, Katsuyama M, Kakehi T, Sasaki M, Ikami K, Zhu K, Yabe-Nishimura C (2009) NADPH oxidase isoforms and anti-hypertensive effects of atorvastatin demonstrated in two animal models. J Pharmacol Sci 111: 260–268.

Dechend R, Fiebeler A, Park JK, Muller DN, Theuer J, Mervaala E, Bieringer M, Gulba D, Dietz R, Luft FC, Haller H (2001) Amelioration of angiotensin II-induced cardiac injury by a 3-hydroxy-3-methylglutaryl coenzyme a reductase inhibitor. Circulation 104: 576–581.

Giordano FJ (2005) Oxygen, oxidative stress, hypoxia, and heart failure. J Clin Invest 115: 500–508.

Habibi J, Whaley-Connell A, Qazi MA, Hayden MR, Cooper SA, Tramontano A, Thyfault J, Stump C, Ferrario C, Muniyappa R, Sowers JR (2007) Rosuvastatin, a 3-hydroxy-3-methyl-glutaryl coenzyme a reductase inhibitor, decreases cardiac oxidative stress and remodeling in Ren2 transgenic rats. Endocrinology 148: 2181–2188.

Hori M, Nishida K (2009) Oxidative stress and left ventricular remodelling after myocardial infarction. Cardiovasc Res 81: 457–464.

Kuroda J, Ago T, Matsushima S, Zhai P, Schneider MD, Sadoshima J (2010) NADPH oxidase 4 (Nox4) is a major source of oxidative stress in the failing heart. Proc Natl Acad Sci 107: 15565–15570.

Kuroda J, Sadoshima J (2010) NADPH oxidase and cardiac failure. J Cardiovasc Transl Res 3: 314–320.

Lambeth JD (2004) NOX enzymes and the biology of reactive oxygen. Nat Rev Immunol 4: 181–189.

Lee TM, Lin MS, Tsai CH, Chang NC (2006) Effect of pravastatin on left ventricular mass in the two-kidney, one-clip hypertensive rats. Am J Physiol Heart 291: H2705–H2713.

Looi YH, Grieve DJ, Siva A, Walker SJ, Anilkumar N, Cave AC, Marber M, Monaghan MJ, Shah AM (2008) Involvement of Nox2 NADPH oxidase in adverse cardiac remodeling after myocardial infarction. Hypertension 51: 319–325.

Maejima Y, Kuroda J, Matsushima S, Ago T, Sadoshima J (2011) Regulation of myocardial growth and death by NADPH oxidase. J Mol Cell Cardiol 50: 408–416.

Martyn KD, Frederick LM, von Loehneysen K, Dinauer MC, Knaus UG (2006) Knaus UG. Functional analysis of Nox4 reveals unique characteristics compared to other NADPH oxidases. Cell Signal 18: 69–82.

Murdoch CE, Zhang M, Cave AC, Shah AM (2006) NADPH oxidase-dependent redox signalling in cardiac hypertrophy, remodelling and failure. Cardiovasc Res 71: 208–215.

Nabeebaccus A, Zhang M, Shah AM (2011) NADPH oxidases and cardiac remodelling. Heart Fail Rev 16: 5–12.

Polizio AH, Balestrasse KB, Yannarelli GG, Noriega GO, Gorzalczany S, Taira C, Tomaro ML (2008) Angiotensin II regulates cardiac hypertrophy via oxidative stress but not antioxidant enzyme activities in experimental renovascular hypertension. Hypertens Res 31: 325–334.

Schiffrin EL (2002) Vascular and cardiac benefits of angiotensin receptor blockers. Am J Med 113: 409–418.

Sedeek M, Hébert RL, Kennedy CR, Burns KD, Touyz RM (2009) Molecular mechanisms of hypertension: role of Nox family NADPH oxidases. Curr Opin Nephrol Hypertens 18: 122–127.

Sicard P, Delemasure S, Korandji C, Segueira-Le Grand A, Lauzier B, Guilland JC, Duvillard L, Zeller M, Cottin Y, Vergely C, Rochette L (2008) Anti-hypertensive effects of Rosuvastatin are associated with decreased inflammation and oxidative stress markers in hypertensive rats. Free Radic Res 42: 226–236.

Sumimoto H, Miyano K, Takeya R (2005) Molecular composition and regulation of the nox family NAD(P)H oxidases. Biochem Biophys Res Commun 338: 677–686.

Sun ZJ, Zhang ZE (2005) Historic perspectives and recent advances in major animal models of hypertension. Acta Pharmacol Sin 26: 295–301.

Tajima N, Kurata H, Nakaya N, Mizuno K, Ohashi Y, Kushiro T, Teramoto T, Uchiyama S, Nakamura H (2008) Pravastatin reduces the risk for cardiovascular disease in Japanese hypercholesterolemic patients with impaired fasting glucose or diabetes: diabetes subanalysis of the Management of Elevated Cholesterol in the Primary Prevention Group of Adult Japanese (MEGA) Study. Atherosclerosis 199: 455–462.

Takimoto E, Kass DA (2007) Role of oxidative stress in cardiac hypertrophy and remodeling. Hypertension 49: 241–248.

Takayama T, Wada A, Tsutamoto T, Ohnishi M, Fujii M, Isono T, Horie M (2004) Contribution of vascular NAD(P)H oxidase to endothelial dysfunction in heart failure and the therapeutic effects of HMG-CoA reductase inhibitor. Circ J 68: 1067–1075.

Thone-R C, Olivier J, Godes M, Zart R, George I, Bauer C, Neumayer HH, Hocher B (2003) Effects of angiotensin-converting enzyme inhibition and calcium channel blockade on cardiac apoptosis in rats with 2K1C (two-kidney/one-clip) renovascular hypertension. Clin Sci (Lond) 104: 79–85.

Wang P, Tang F, Li R, Zhang H, Chen S, Liu P, Huang H (2007) Contribution of different Nox homologues to cardiac remodeling in two-kidney two-clip renovascular hypertensive rats: Effect of valsartan. Pharmaco Res 55: 408–417.

Weber KT (1997) Extracellular matrix remodeling in heart failure: a role for de novo angiotensin II generation. Circulation 96: 4065–4082.

Wang P, Wu X, Bao Y, Fang J, Zhou S, Gao J, Pi R, Mou YG, Liu P (2011) Tanshinone IIA prevents cardiac remodeling through attenuating NAD (P)H oxidase-derived reactive oxygen species production in hypertensive rats. Pharmazie 66: 517–524.

Whaley-Connell A, Habibi J, Nistala R, Cooper SA, Karuparthi PR, Hayden MR, Rehmer N, DeMarco VG, Andresen BT, Wei Y, Ferrario C, Sowers JR (2008) Attenuation of NADPH oxidase activation and glomerular filtration barrier remodeling with statin treatment. Hypertension 51: 474–480.

Xu Z, Okamoto H, Akino M, Onozuka H, Matsui Y, Tsutsui H (2008) Pravastatin attenuates left ventricular remodeling and diastolic dysfunction in angiotensinII-induced hypertensive mice. J Cardiovasc Pharmacol 51: 62–70.

Zhang H, Pi R, Li R,Wang P, Tang F, Zhou S, Gao J, Jiang J, Chen S, Liu P (2007) PPARbeta/delta activation inhibits angiotensin II-induced collagen type I expression in rat cardiac fibroblasts, Arch Biochem Biophys 460: 25–32.

Zhang M, Brewer AC, Schröder K, Santos CX, Grieve DJ, Wang M, Anilkumar N, Yu B, Dong X, Walker SJ, Brandes RP, Shah AM (2010) NADPH oxidase-4 mediates protection against chronic load-induced stress in mouse hearts by enhancing angiogenesis. Proc Natl Acad Sci 107: 18121–18126.

Zhao H, Liao Y, Minamino T, Asano Y, Asakura M, Kim J, Asanuma H, Takashima S, Hori M, Kitakaze M (2008) Inhibition of cardiac remodeling by pravastatin is associated with amelioration of endoplasmic reticulum stress. Hypertens Res 31: 1977–1987.

Zhou SG, Zhou SF, Huang HQ, Chen JW, Huang M, Liu PQ (2006) Proteomic analysis of hypertrophied myocardial protein patterns in renovascularly hypertensive and spontaneously hypertensive rats. J Proteome Res 5: 2901–2908.